Liquid Crystals
Publication details, including instructions for authors and subscription information:
http://www.informaworld.com/smpp/title~content=t713926090

Rod-like liquid crystals of organic transition metal complexes. I. Reversible transformation between blue smectogen and red nematogen

Kazuchika Ohta[a]; Hiroshi Ema[a]; Yasue Morizumi[a]; Takuya Watanabe[a]; Tetsuya Fujimoto[a]; Iwao Yamamoto[a]
[a] Department of Functional Polymer Science, Faculty of Textile Science and Technology, Shinshu University, Ueda, Japan

To cite this Article Ohta, Kazuchika , Ema, Hiroshi , Morizumi, Yasue , Watanabe, Takuya , Fujimoto, Tetsuya and Yamamoto, Iwao(1990) 'Rod-like liquid crystals of organic transition metal complexes. I. Reversible transformation between blue smectogen and red nematogen', Liquid Crystals, 8: 3, 311 — 330

To link to this Article: DOI: 10.1080/02678299008047350

URL: http://dx.doi.org/10.1080/02678299008047350

LIQUID CRYSTALS, 1990, VOL. 8, NO. 3, 311–330

Rod-like liquid crystals of organic transition metal complexes

I. Reversible transformation between blue smectogen and red nematogen

by KAZUCHIKA OHTA, HIROSHI EMA, YASUE MORIZUMI,
TAKUYA WATANABE, TETSUYA FUJIMOTO and IWAO YAMAMOTO
Department of Functional Polymer Science, Faculty of Textile Science and
Technology, Shinshu University, Ueda 386, Japan

(*Received 16 September 1989; accepted 5 March 1990*)

Two novel types of transition-metal-containing liquid crystals, bis(*p*-*n*-alkoxydithiobenzoato)nickel(II) (abbreviated as $(C_nO\text{–DTB})_2Ni$), and (*p*-*n*-alkoxydithiobenzoato)(*p*-*n*-alkoxyperthiobenzoato)nickel(II) (abbreviated as $(C_nO\text{–DTB})(C_nO\text{–PTB})Ni$), were synthesized. It was found that the $(C_nO\text{–DTB})_2Ni$ complex for $n = 8$ has *smectic* H and C mesophases, and that the $(C_nO\text{–DTB})_2Ni$ complexes for $n = 4$ and 8 easily transform into the corresponding monoperthio complexes, $(C_nO\text{–DTB})(C_nO\text{–PTB})Ni$, by heating at temperatures between 230°C and 285°C. It was confirmed that the transformation originates from an intermolecular reaction between the $(C_nO\text{–DTB})_2Ni$ complexes at high temperatures, and that the origin of the extra sulphurs in the resulting $(C_nO\text{–DTB})(C_nO\text{–PTB})Ni$ complexes is the neighbouring $(C_nO\text{–DTB})_2Ni$ complexes. Interestingly, each of the $(C_nO\text{–DTB})(C_nO\text{–PTB})Ni$ complexes ($n = 4$ and 8), has *nematic* mesophase and exhibits a unique double melting behaviour via the nematic phase, which is the first example in liquid crystals. The reversible transformation between the *blue smectic rod-like* $(C_nO\text{–DTB})_2Ni$ complex and the *red nematic* Λ*-like* $(C_nO\text{–DTB})(C_nO\text{–PTB})Ni$ complex is possible.

1. Introduction

Organic transition metal complexes substituted with long alkyl chains are interesting target molecules for the study of the physical properties which cannot be observed in the unsubstituted core complexes. In these long-chain-substituted complexes, six properties have been reported: (1) good solubility in alkanes [1, 2], (2) micelle formation [3] and Langmuir–Blodgett film formation [4], (3) unusual thermochromism [2], (4) double melting behaviour [5], (5) mesomorphism [6], and (6) gelation [7]. During our investigation of novel transition-metal-containing liquid crystals [8], we discovered new types of sulphur-ligand nickel(II) complexes, **1**, **2**, and **3** (formulae).

Previously, we reported that each of the complexes **1** ($n = 9, 11, 12$) exhibits *monotropic* smectic mesomorphism [9]. In order to obtain *enantiotropic* mesophases in this system, we introduced phenyl rings into the complex **1** to yield the complex **2**. It was found that this complex **2** has enantiotropic smectic H and C mesophases for $n = 8$. Furthermore, the long chain substituted bis(dithiobenzoato)nickel(II) complex **2** easily transforms into the corresponding (dithiobenzoato)(perthiobenzoato)-nickel(II) complex **3** by heating the complex **2** at temperatures between 230°C and 285°C. It originates from an intermolecular reaction of complexes **2** at high temperatures. Interestingly, each of the complexes **3** has a nematic mesophase and exhibits "unusual

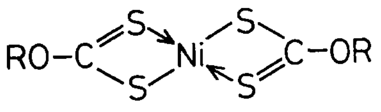

1 n = 9, 11, 12

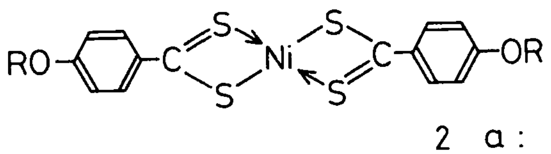

2 a : n = 4
b : n = 8

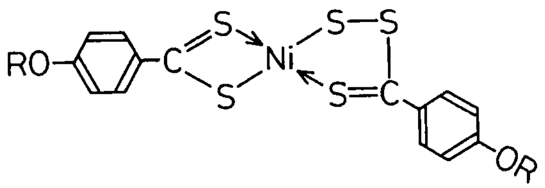

3 a : n = 4
b : n = 8

$R = C_nH_{2n+1}$

double melting behaviour" [10] via the nematic phase. We wish to report here these interesting properties of the complexes **2** and **3**.

2. Results and discussion

Bis(*p*-*n*-alkoxydithiobenzoato)nickel(II) complexes, **2**, were prepared by a modification of the method of Bost and Mattox [11]. The phase transition behaviour of the complexes, **2a,b** and **3a,b**, is summarized in table 1. Three of them, **2b** and **3a,b**, exhibit mesomorphism.

2.1. *Microscopic observations of the phase transition behaviour for* $(C_8O\text{-}DTB)_2Ni$, ***2b***, *below 230°C*

When the strip-like virgin crystals of **2b** were heated from room temperature at 10°C/min, the crystalline phase (K) transformed into a rigid mesophase (M_1) at 155°C. The M_1 phase exhibited highly viscous fluidity when a sample of the M_1 phase was pressed at 160°C. On further heating another mesophase (M_2) appeared at 189°C, exhibiting spontaneous fluidity and a schlieren texture (figure 1 (*c*)). On cooling the mesophase M_2 from 200°C at − 10°C/min, the schlieren texture changed into a mosaic texture at 186–182°C (figure 1 (*b*)). On further cooling the mosaic-textured mesophase (M_1) was abruptly crystallized at 112°C (figure 1 (*a*)). When the crystals were heated again from 100°C at 10°C/min, the mosaic texture appeared again at 155°C and the schlieren texture at 189°C. Hence, the mesophases M_1 and M_2 in complex **2b** are enantiotropic.

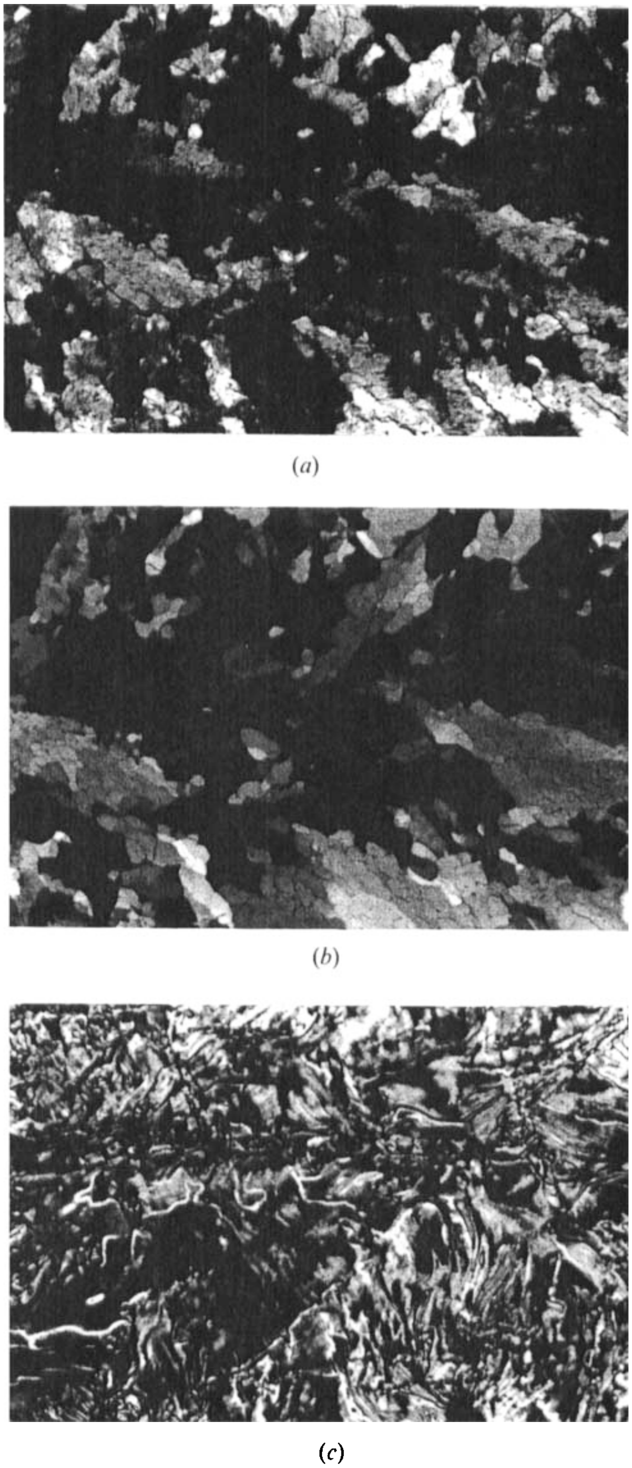

Figure 1. Photomicrographs of the mesophases in the $(C_8O\text{–}DTB)_2Ni$ complex, **2b**: (*a*) the crystalline phase (K) at room temperature, (*b*) the M_1 mesophase (smectic H phase) at 170°C, and the M_2 mesophase (smectic C phase) at 210°C.

Table 1. Phase transition temperatures (T) and enthalpy changes (ΔH) of the dithiolato complex derivatives, **2a,b** and **3a,b**.

Complex	$\text{Phase} \xrightarrow{T{}^{\circ}\text{C}[\Delta H\,\text{kJ mol}^{-1}]} \text{Phase}$†
2a: $(C_4O\text{-}DTB)_2Ni$§	$K_1 \xrightarrow{164[5\cdot73]} K_2 \xrightarrow{242[39\cdot8]}$ ‡
2b: $(C_8O\text{-}DTB)_2Ni$	$K \underset{112}{\overset{155[16\cdot9]}{\rightleftharpoons}} S_H \underset{186\text{–}182}{\overset{189[17\cdot2]}{\rightleftharpoons}} S_C \overset{c.\,230}{\rightleftharpoons}$ ‡
3a: $(C_4O\text{-}DTB)(C_4O\text{-}PTB)Ni$‖	$\begin{tikzcd} K_1 \arrow[r, "c.\,132"] \arrow[dr, "139"'] & K_2 \arrow[r, "145[40\cdot2]"] & N \arrow[r, "242[0\cdot59]"] \arrow[ll, bend right, "c.\,117"'] & \text{I.L. (decomp.)} \\ & N \arrow[u, squiggly, "\text{slow}"'] & & \end{tikzcd}$
3b: $(C_8O\text{-}DTB)(C_8O\text{-}PTB)Ni$¶	$\begin{tikzcd} K_1 \arrow[r, "c.\,89"] \arrow[dr, "116\cdot5"'] & K_2 \arrow[r, shift left, "128[39\cdot8]"] & N \arrow[l, shift left, "c.\,98"] \arrow[r, shift left, "200[0\cdot75]"] \arrow[ll, bend right, "c.\,98"'] & \text{I.L.} \arrow[l, shift left, "200"] \\ & N \arrow[u, squiggly, "\text{fast}"'] & & \end{tikzcd}$

† Phase nomenclature; K = crystal, S = smectic, N = nematic, and I.L. = isotropic liquid.

‡ The transformation from **2** to **3** takes place as mentioned in the main text.

§ The virgin sample is the K_1 crystalline phase.

‖ The virgin sample is the K_2 crystalline phase.

¶ The virgin sample is a mixture of K_1 and K_2 crystalline phases.

2.2. *X-ray analyses of the M_1 and M_2 mesophases in the $(C_8O\text{-}DTB)_2$ Ni complex*

X-ray diffraction powder patterns (figure 2 and table 2) were measured for the following three states; (*a*) the virgin crystals (K) at room temperature, (*b*) the M_1 mesophase at 170°C, and (*c*) the M_2 mesophase at 210°C.

Comparing the patterns of (*b*) and (*c*) with that of (*a*), these powder patterns lack the diffraction peaks for the high Bragg angles ($2\theta > 25°$) although the pattern (*a*) of the K phase show these peaks. This result means that the orders of the M_1 and the M_2 phases are reduced from that of the crystal K. Comparing the pattern of (*c*) with (*b*), the pattern (*c*) shows a diffuse element of *c*. 4·6 Å ($2\theta \doteqdot 19$) and, on the other

Table 2. X-ray diffraction data for the M_1 and M_2 mesophases in the $(C_8O\text{-}DTB)_2Ni$ complex, **2b**.

	$M_1(S_H)$ at 170°C			$M_2(S_C)$ at 210°C	
$d_{obs.}$/Å	$d_{calc.}$/Å	(hkl)	$d_{obs.}$/Å	$d_{calc.}$/Å	(hkl)
25·14	25·14	(0 0 1)	25·45	25·45	(0 0 1)
12·57	12·57	(0 0 2)	12·73	12·73	(0 0 2)
8·35	8·38	(0 0 3)	8·43	8·48	(0 0 3)
5·15	5·15	$(1\,1\,\bar{1})$	*c*. 4·6	–	–
4·99	4·99	(1 1 0)			
4·62	4·66 4·62	(1 1 1) (2 0 0)		$c = 25\cdot45$ Å	
4·11	4·20	(2 0 1)			
3·91	3·82	$(2\,1\,\bar{1})$			
	$a = 10\cdot5$ Å $b = 5.92$ Å $c = 28\cdot7$ Å $\beta = 119°$				

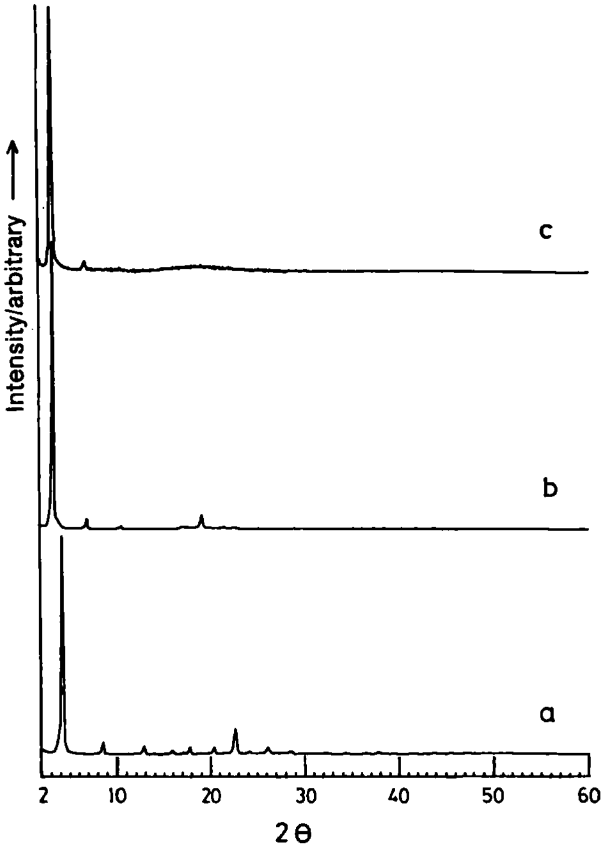

Figure 2. X-ray diffraction powder patterns of the phases in the $(C_8O\text{-}DTB)_2Ni$ complex, **2b**: (*a*) the crystalline phase (K) at room temperature, (*b*) the M_1 mesophase (smectic H phase) at 170°C, and the M_2 mesophase (smectic C phase) at 210°C.

hand, the pattern of (*b*) gives four narrow reflections with a very small diffuse element in the region of $2\theta = 17 \sim 23°$. Furthermore, each of the patterns of (*b*) and (*c*) shows the three narrow reflections for the low Bragg angles and their spacings are exactly in the ratio 1 : 1/2 : 1/3, which is a characteristic of lamellar structure. Hence, pattern (*c*) is consistent with the layered structure with the random arrangement within the layers, which corresponds to a smectic A phase or a smectic C phase. As mentioned previously the M_2 phase gave the schlieren texture. Since a smectic A phase does not give a schlieren texture, the M_2 phase can be assigned as a smectic C phase. On the other hand, the pattern of (*b*) is compatible with the layered structure with the three-dimensional ordering, which corresponds to a smectic G phase or a smectic H phase. Both the smectic G phase and the smectic H phase have monoclinic lattices. However, a smectic G phase has a pseudo-hexagonal close packing in the layers, while a smectic H phase has an orthorhombic (rectangular) close packing in the layers [12]. Therefore, the powder pattern of a smectic G phase gives two very close reflections corresponding to the spacings of (110) and (200), while the pattern of a smectic H phase gives two separated reflections corresponding to the spacings of (110) and (200) [13]. When the spacings at 25·14 Å, 5·15 Å, 4·99 Å and 4·26 Å in the M_1 phase are assumed to be (001), $(11\bar{1})$, (110), and (200) lines in a monoclinic lattice, respectively, these calculated values are in fair agreement with the observed values as summarized in table 2. The lattice constants become $a = 10{\cdot}5$ Å, $b = 5{\cdot}92$ Å, $c = 28{\cdot}7$ Å and $\beta = 119°$. Furthermore, the spacings corresponding to (110) and (200) reflections are well separated. Therefore, we concluded that the M_1 phase is a smectic H phase.

Thus, X-ray diffraction powder patterns of the mesophases in $(C_8O\text{–}DTB)_2Ni$ at 170°C and 210°C revealed that the M_1 phase is a smectic H and the M_2 phase is a smectic C.

2.3. *Microscopic observations of the phase transition behaviour for the sample heated over 230°C*

When the smectic C (M_2) phase of **2b** was heated above *c.* 230°C at 20°C/min, the phase cleared into a red isotropic liquid (IL) at 245–255°C. Cooling the red IL from 255°C at −20°C/min, many droplets which are a characteristic texture of the nematic phase appeared at 142°C and all areas were covered with schlieren texture at 131°C. On further cooling, the red nematic phase was crystallized into red and yellow spherulites at *c.* 86°C. When the spherulites were heated from room temperature at 20°C/min, the yellow spherulites transformed into the red spherulites at 116°C and the red nematic phase appeared at 116–130°C, the nematic phase gradually cleared into the red IL at 140–162°C. Thus, once the complex **2b** is heated over 245–255°C, it does not show

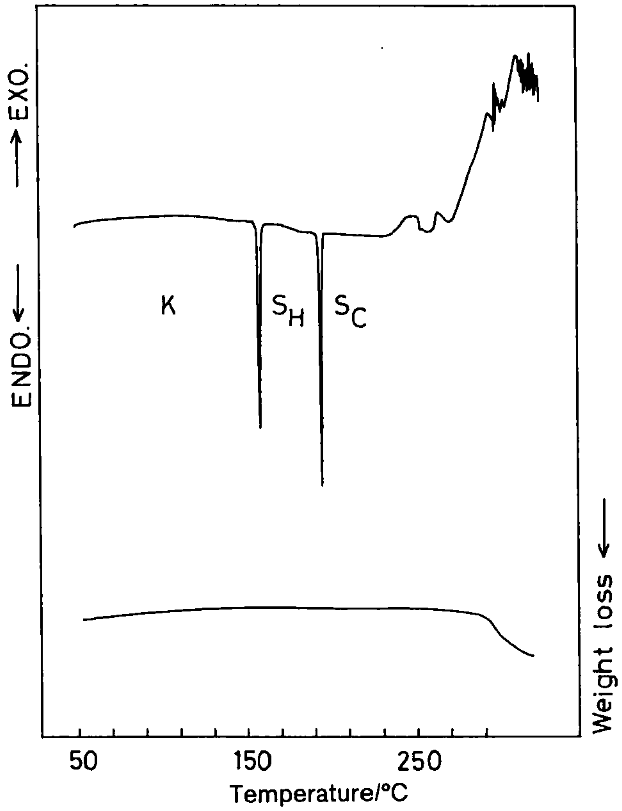

Figure 3. Thermogravity analysis and differential scanning calorimetry (TG-DSC) thermograms of the $(C_8O\text{–}DTB)_2Ni$ complex, **2b**.

the original smectic mesomorphism but nematic mesomorphism. The differential scanning calorimetry (DSC) thermogram of the virgin sample of complex **2b** was not smooth over *c*. 230°C without a weight loss. The weight loss could not be observed until *c*. 285°C (figure 3).

2.4. *Identification of the product of the heated sample by means of spectroscopic techniques*

The infrared spectrum of the sample heated at 230°C for 1·5 hours is different from that of the virgin sample of complex **2b** (figure 4). In this IR spectrum 530–570 cm^{-1} bands of the heated sample of **2b** suggest a formation of a perthiobenzoato derivative, judging from the far-infrared spectra in figure 3 of the paper by Fackler *et al.* [14]. The Ni–S stretching mode of the virgin sample of **2b** is observed at 370 cm^{-1} but this mode disappears in the heated sample of **2b** (figure 4), which is compatible with the far-infrared spectra of (A) bis(dithiobenzoato)nickel(II), $Ni(S_2CC_6H_5)_2$, and (B) (dithiobenzoato)(perthiobenzoato)nickel(II), $Ni(S_2CC_6H_5)(S_3CC_6H_5)$, in figure 3 of Fackler *et al.* [14]. Hence, the changes from the IR spectrum of the virgin sample of **2b** to that of the heated sample of **2b** (figure 4) suggest a transformation from **2b** of bis(*p*-*n*-octyloxydithiobenzoato)nickel(II) (abbreviated as $(C_8O\text{–}DTB)_2Ni$) to **3b** of (*p*-*n*-octyloxydithiobenzoato)(*p*-*n*-octyloxyperthiobenzoato)nickel(II) (abbreviated as $(C_8O\text{–}DTB)(C_8O\text{–}PTB)Ni$) with an intermolecular reaction between the $(C_8O\text{–}DTB)_2Ni$ complexes at the high temperature.

To confirm this transformation the visible spectrum of the virgin $(C_8O\text{–}DTB)_2Ni$ complex and that of the heated sample have been recorded (figure 5), because

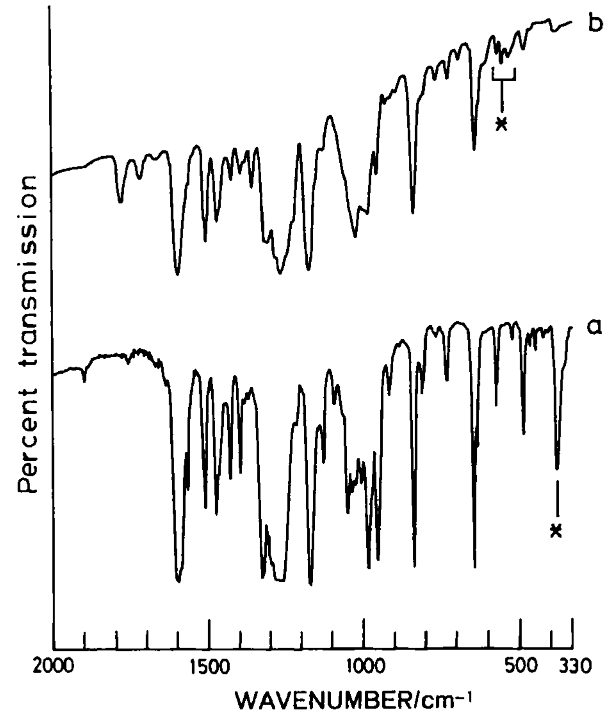

Figure 4. Infrared spectra of (*a*) the virgin sample of the $(C_8O\text{–}DTB)_2Ni$ complex and (*b*) the heated $(C_8O\text{–}DTB)_2Ni$ sample at 230°C for 1·5 hours. KBr pellets.

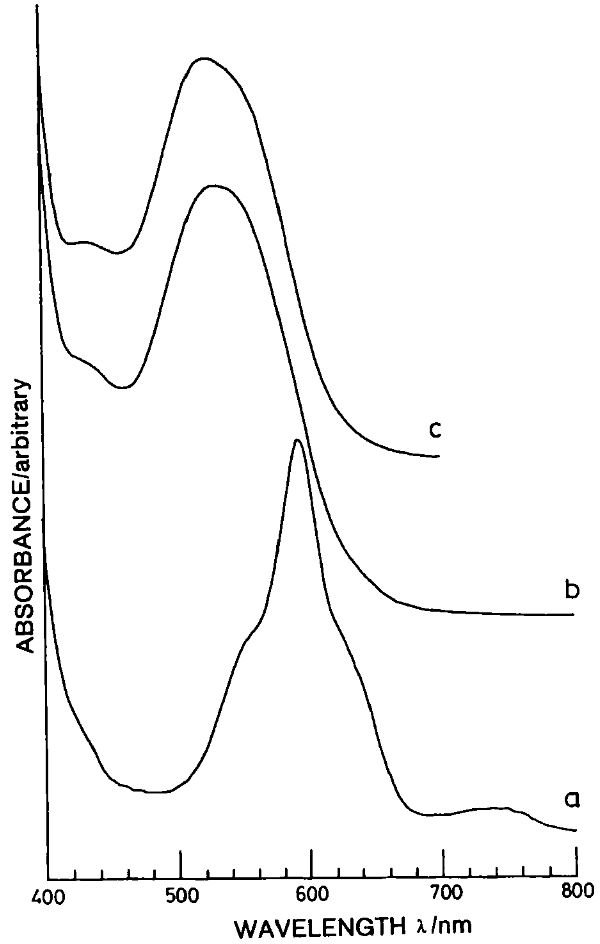

Figure 5. Visible absorption spectra in $CHCl_3$: (*a*) the virgin sample of the $(C_8O\text{-}DTB)_2Ni$ complex, **2b**; (*b*) the heated $(C_8O\text{-}DTB)_2Ni$ sample at 230°C for 1 hour; (*c*) the chemically pure sample of the $(C_8O\text{-}DTB)(C_8O\text{-}PTB)Ni$ complex, **3b**.

Fackler *et al.* mentioned that "the visible spectra of the nickel(II) dithioaryl acid, mixed-ligand, and perthioaryl acid complexes are sufficiently different to use these data for identification purposes" [14]. The spectrum of the virgin sample of the present $(C_8O\text{-}DTB)_2Ni$ complex (figure 5(*a*)) is compatible with that of the core complex, $Ni(S_2CC_6H_5)_2$, in figure 2 of Fackler *et al.* [14]. On the other hand, the spectrum of the present heated sample (figure 5(*b*)) is compatible with that of the unsubstituted monoperthio (mixed-ligand) complex, $Ni(S_2CC_6H_5)(S_3CC_6H_5)$, of Fackler *et al.* [14]. Recrystallization of the heated sample of **2b** was carried out from *n*-hexane to obtain the pure monoperthio complex **3b**, $(C_8O\text{-}DTB)$ $(C_8O\text{-}PTB)Ni$. The λ_{max} at 526 nm of the chemically pure monoperthio complex **3b** (figure 5(*c*)) is the same as that of the unsubstituted monoperthio complex, Ni(dtb)(dtbs), of Furlani *et al.* [15].

For the chemically pure monoperthio complex **3b**, the 250 MHz FT-^{1}H-NMR spectrum was recorded (figure 6(*b*)). It shows two distinct triplets of $-OCH_2-$ separated by 11·5 Hz in $CDCl_3$. This is consistent with the presence of two electronically

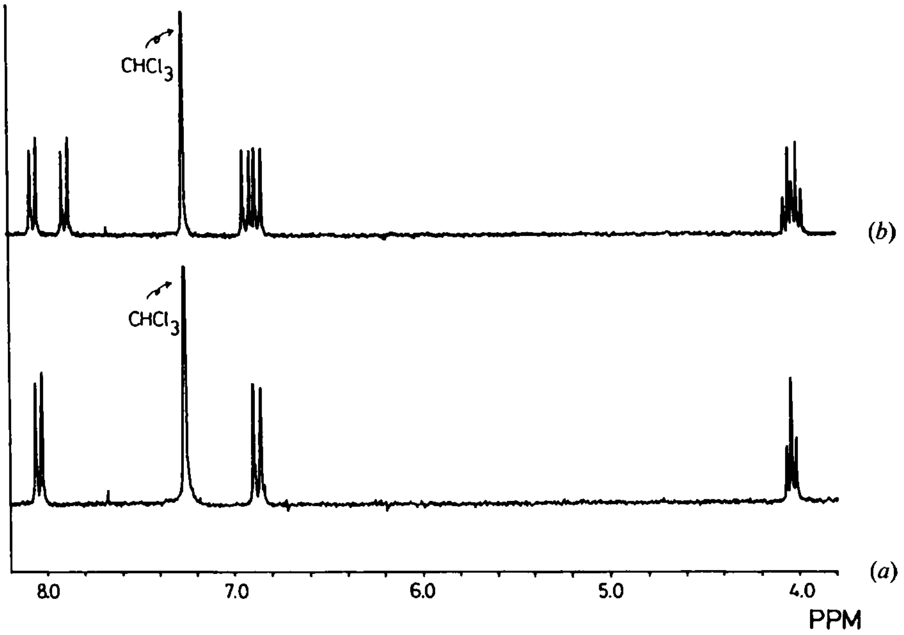

Figure 6. ^{1}H-NMR spectra in $CDCl_3$: (*a*) the (C_8O–DTB)$_2$Ni complex, **2b**; (*b*) the (C_8O–DTB)-(C_8O–PTB)Ni complex, **3b**.

different $-OCH_2-$ groups. On the other hand, the spectrum (figure 6(*a*)) of the bis(*p*-*n*-octyloxydithiobenzoato)nickel(II) complex, (C_8O–DTB)$_2$Ni, **2b** shows only one triplet of $-OCH_2-$. This fact is consistent with the ^{1}H-NMR spectrum of bis(*p*-dithiotoluato)nickel(II) reported by Fackler *et al.* [16].

Thus, the formation from bis(*p*-*n*-octyloxydithiobenzoato)nickel(II) **2b** to the monoperthio complex **3b** by heating has been confirmed using infrared, visible, and ^{1}H-NMR spectra.

2.5. *The origin of the extra sulphur in the monoperthio complex 3b*

The monoperthio transformation is not due to oxygen in the air. As shown in figure 7(*a*)–(*c*), both visible spectra of the sample heated in a *nitrogen* atmosphere at 250°C (figure 7(*b*)) and the sample heated in an *oxygen* atmosphere at 250°C (figure 7(*c*)) are the same as that of the chemically pure monoperthio complex **3b** obtained from recrystallization (figure 7(*a*)). Hence, there is no influence of oxygen on this monoperthio transformation. The transformation must originate from an intermolecular reaction between the (C_8O–DTB)$_2$Ni complexes because there is no source of the extra sulphur except for the (C_8O–DTB)$_2$Ni complexes themselves. While a detailed mechanism is not warranted at this time, the scheme given in figure 8 is consistent with the studies of Fackler *et al.* on the mechanism of the radioactive sulphur-35 addition to $Ni(CS_3)_2^{2-}$ [17]. The extra sulphur in the monoperthio complex was easily abstracted in the chloroform solution by the addition of PPh_3 to give the original bis(*p*-*n*-octyloxydithiobenzoato)nickel(II) complex. This fact is clearly shown by the visible spectrum change in figure 7(*d*). This is consistent with the studies of Fackler *et al.* on the sulphur abstraction reaction of (dithiobenzoato)(perthiobenzoato)nickel(II) with PPh_3 [16]. Hence, we have concluded that the monoperthio

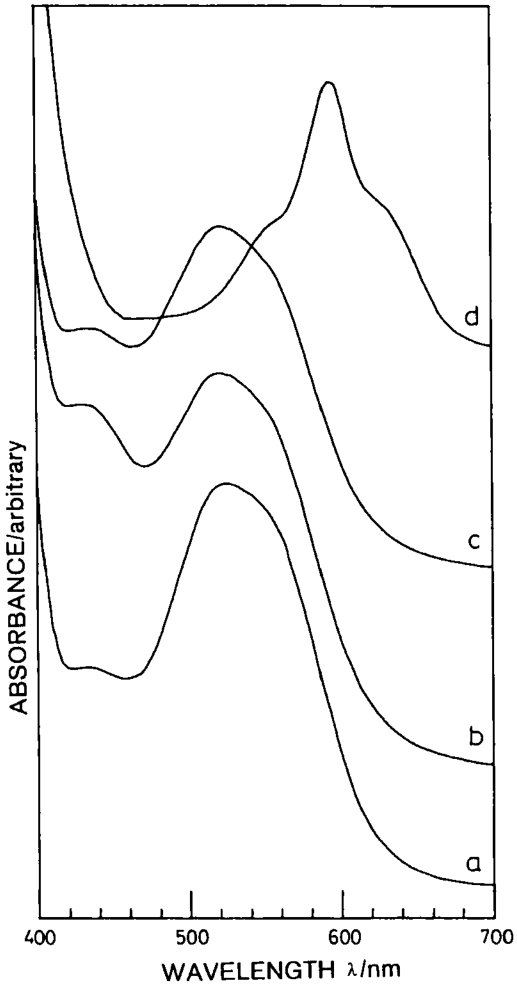

Figure 7. Visible absorption spectra in $CHCl_3$: (*a*) the chemically pure (C_8O-DTB)-(C_8O-PTB)Ni complex, **3b**; (*b*) the heated $(C_8O\text{-DTB})_2Ni$ complex in an oxygen atmosphere at 250°C for 1 hour; (*c*) the heated $(C_8O\text{-DTB})_2Ni$ complex in a nitrogen atmosphere at 250°C for 1 hour; (*d*) the chloroform solution of **3b** after adding triphenylphosphine.

transformation originates from an intermolecular reaction between the $(C_8O\text{-DTB})_2Ni$ complexes, and that the origin of the extra sulphur is the neighbouring $(C_8O\text{-DTB})_2Ni$ complexes.

2.6. *Microscopic observations of the phase transition behaviour for the chemically pure (C_8O-DTB)(C_8O-PTB)Ni complex, **3b***

The chemically pure virgin sample of **3b**, which was obtained by recrystallization from *n*-hexane, was very soft powder. When the powder of **3b** was heated from room temperature at 10°C/min, it transformed into strip-like crystals at 101–114°C. On further heating a schlieren texture could be observed at 124°C and long strip-like crystals remained; then the portion of the schlieren texture remained unchanged and the other portion of strip-like crystals changed into the same schlieren texture at *c.* 128°C exhibiting a spontaneous fluidity. Above 128°C we could observe both the schlieren texture and a marbled texture which are a characteristic feature of the

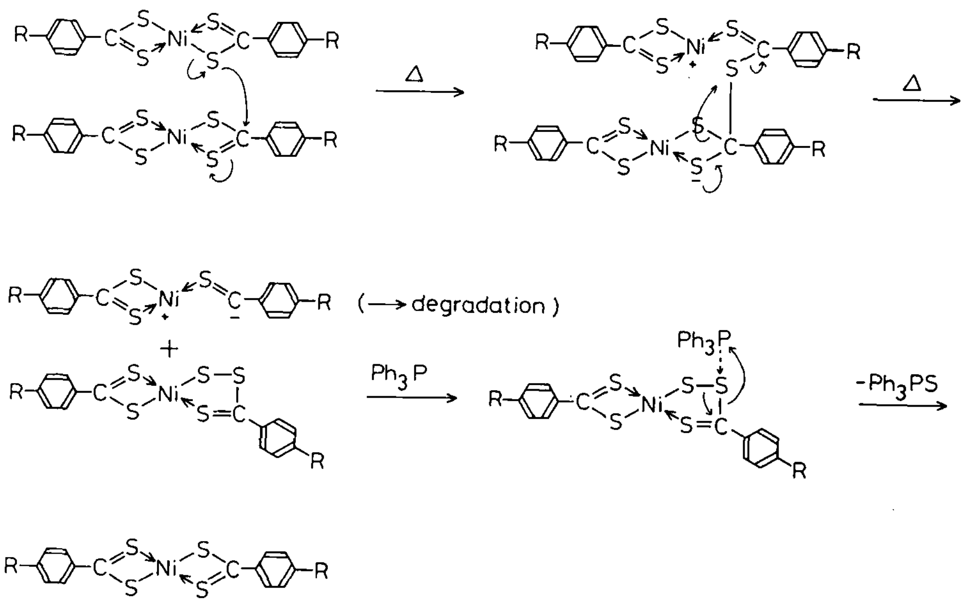

Figure 8. Mechanism of the monoperthio transformation and the sulphur abstraction reaction with triphenylphosphine.

nematic mesophase. On further heating, the nematic phase cleared into a red isotropic liquid at 200°C. When the IL was cooled down from 202°C at −10°C/min, the nematic phase appeared again from the IL at 200°C. A photomicrograph of the red nematic phase at 198·3°C is shown in figure 9. On further cooling, the compound

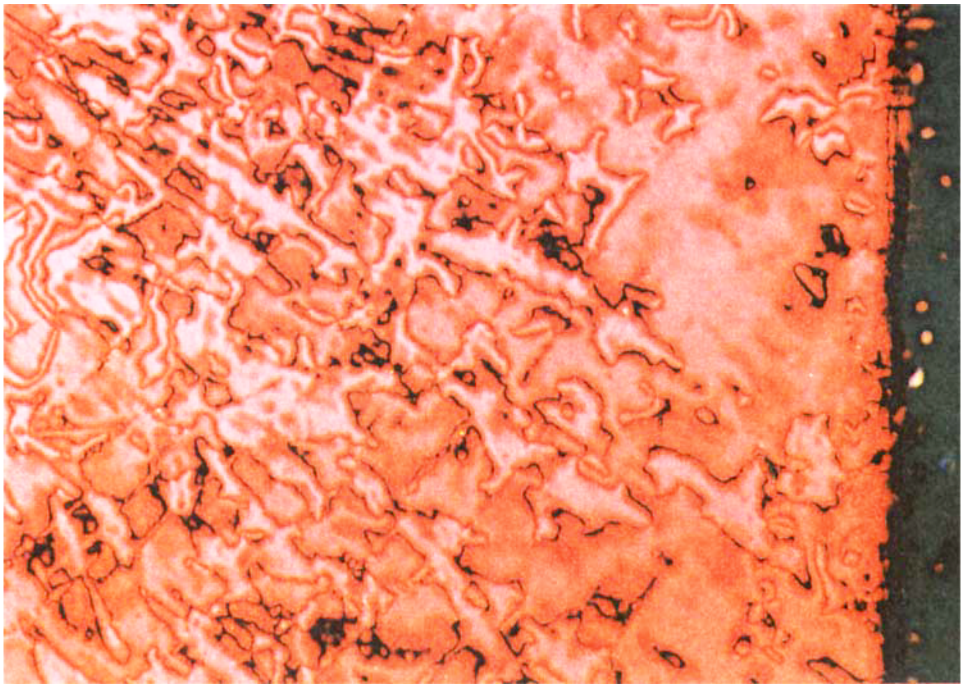

Figure 9. Texture of the red nematic phase of the (C_8O–DTB)(C_8O–PTB)Ni complex, **3b**, at 198·3°C.

abruptly crystallized at 98°C into a small portion of yellow spherulites (K_1) and a large portion of red spherulites (K_2). When a mixture of the yellow spherulites (K_1) and red spherulites (K_2) was heated up from 30·0°C at 10°C/min, the yellow spherulites (K_1) started to transform into red spherulites (K_2) at 89°C. This crystal–crystal phase transition was very slow and continued until *c.* 110°C, i.e. the yellow spherulites (K_1) were superheated until *c.* 110°C. After the complete transition the red spherulites (K_2) did not exhibit fluidity until 128°C; they suddenly started to flow at 128°C exhibiting characteristics of nematic textures, both marble and schlieren. On further heating it cleared into the red isotropic liquid at 200°C. Thus, the nematic phase could be observed enantiotropically between 128°C and 200°C.

2.7. *Double melting behaviour via the nematic phase in* $(C_8O\text{-}DTB)(C_8O\text{-}PTB)Ni$

However, there remained the question that the virgin sample exhibits a schlieren texture at 124°C below the melting point of 128°C. We suspected a double melting behaviour [5, 18] via the nematic mesophase which might be caused by the superheating of the yellow spherulites (K_1) or the virgin soft powder. If the superheating of the yellow spherulites (K_1) continues until the melting point (T_{m_1}) of the yellow spherulites (K_1), a portion of the yellow spherulites (K_1) remains and the melting transition (at T_{m_1}) from the yellow spherulites (K_1) to the nematic phase (N) can be

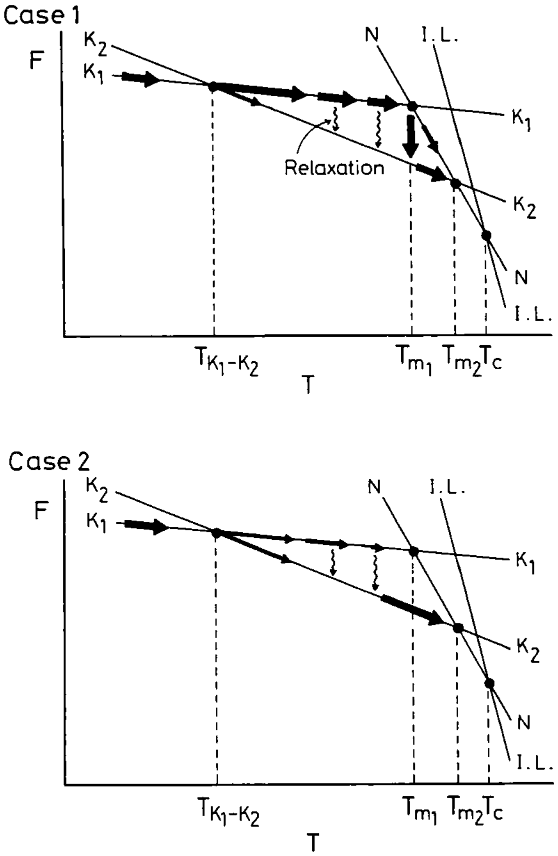

Figure 10. Two cases of the free energy versus temperature (F–T) diagrams; Case 1: double melting behaviour via a nematic phase; Case 2: single melting behaviour.

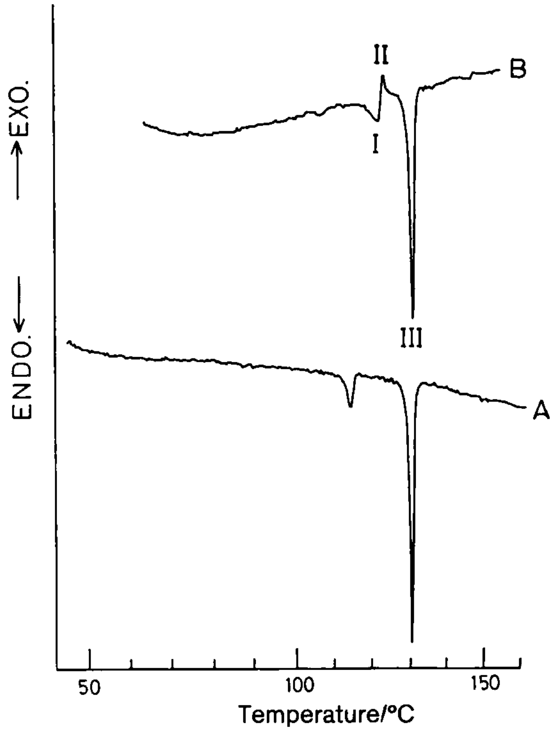

Figure 11. Differential scanning calorimetry (DSC) thermograms of (A) the virgin sample of the $(C_8O\text{-}DTB)_2Ni$ complex and (B) a typical double melting behaviour of the non-virgin sample of this complex. Each of the heating rates was 10°C/min.

observed (Case 1 in figure 10). If both of the crystal–crystal phase transition ($T_{K_1\text{-}K_2}$) and the relaxation from the yellow spherulites (K_1) to the red spherulites (K_2) finish completely before the m.p. (T_{m_1}) of the yellow spherulites (K_1), the melting transition (at T_{m_1}) from K_1 to N cannot be observed (Case 2 in figure 10).

Figure 11 (A) shows the thermogram of differential scanning calorimetry (DSC) for the virgin sample at the heating rate 10°C/min. Two endothermic peaks could be observed at 113°C and 128°C. The peak at 128°C is compatible with the melting point of the red spherulites (K_2) into the nematic phase which could be observed with the microscope. The other endothermic peak did not show a constant temperature; the temperatures of the peak varied between 110°C and 114°C for several thermograms. Hence, the peak corresponds to the crystal–crystal phase transition from the yellow spherulites (K_1) to the red spherulites (K_2) after the variable superheating. The DSC thermogram in figure 11 (A) represents Case 2 mentioned above. After slowly cooling the nematic phase from 160°C to 65°C in the DSC apparatus, it was heated again at 10°C/min from 65°C; a typical thermogram of double melting behaviour [19] could be obtained as shown in figure 11 (B). In this figure, peak I at 116·5°C corresponds to the melting from the yellow spherulites (K_1) to the nematic phase. An exothermic peak II means the recrystallization from the nematic phase to the red spherulites (K_2), and peak III at 128°C shows the melting of the red spherulites (K_2) to the nematic phase. Hence, the DSC thermogram in figure 11 (B) represents Case 1 mentioned previously. Thus the double melting behaviour via the nematic phase has been confirmed by the DSC measurements and the microscopic observations.

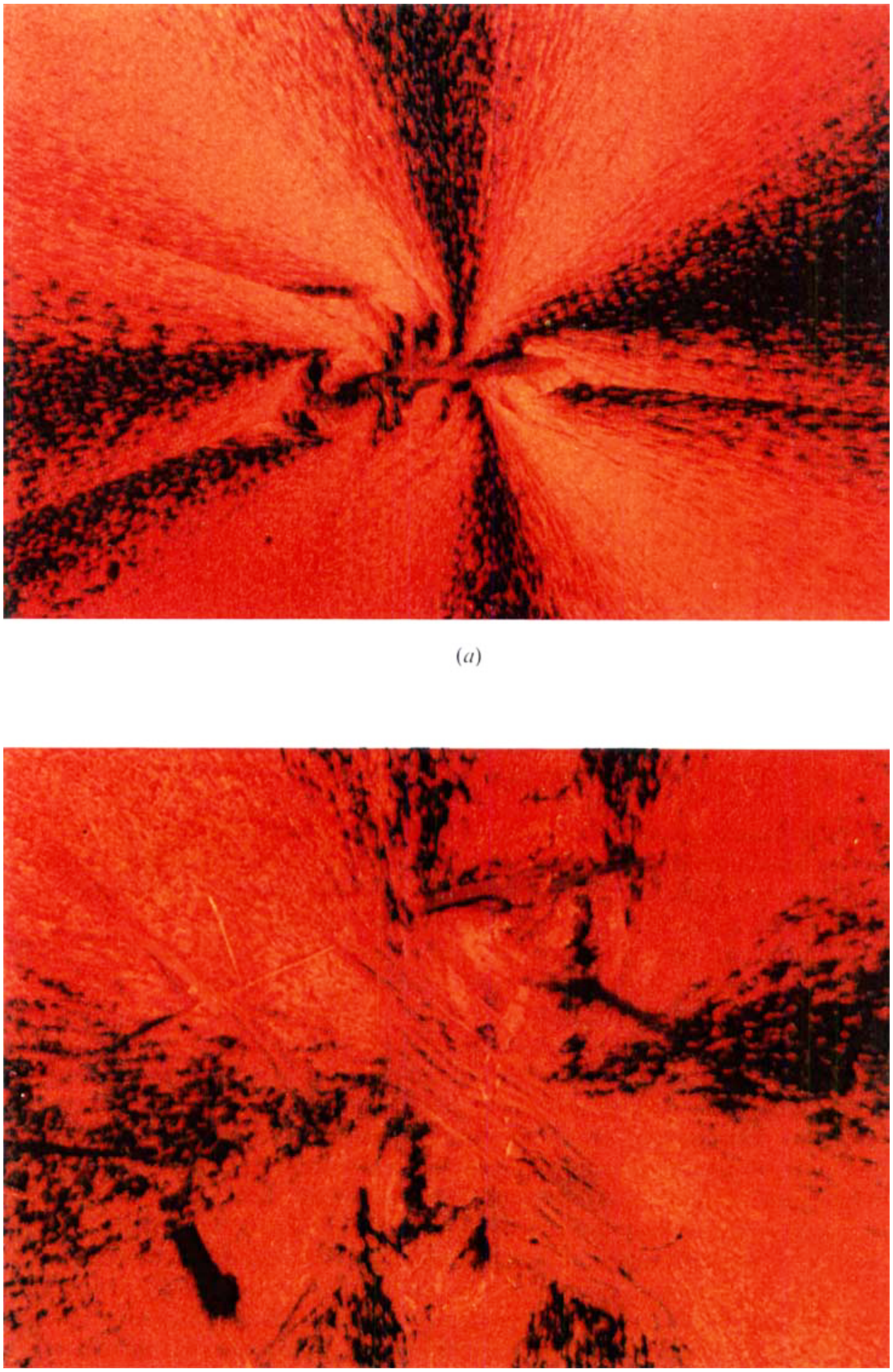

(a)

(b)

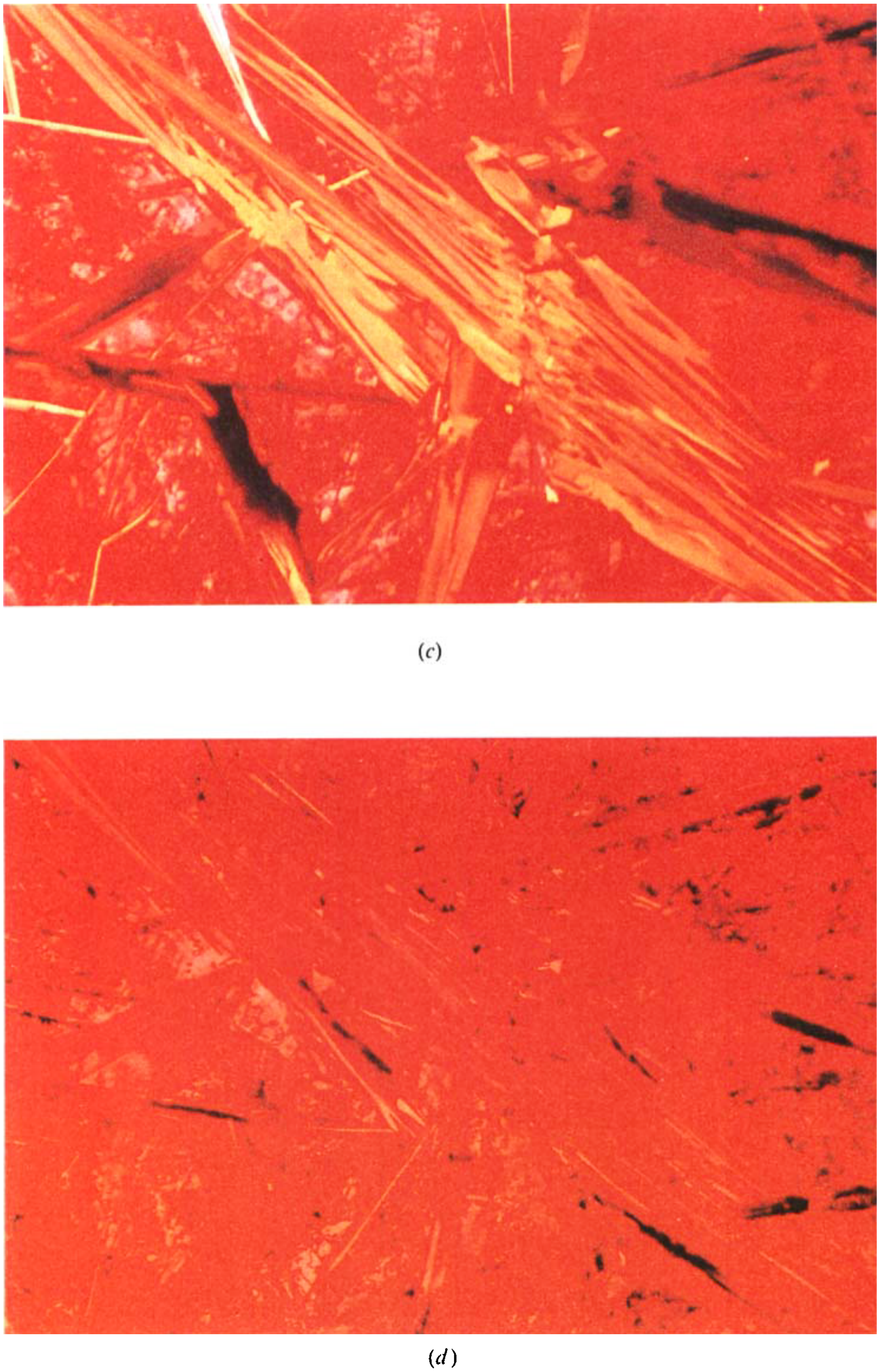

(*c*)

(*d*)

Figure 12. Photomicrographs of unusual double melting behaviour [5] via the nematic phase of the $(C_4O\text{–}DTB)(C_4O\text{–}PTB)Ni$ complex, **3a**. (*a*) r.t., $K_1 + K_2$; (*b*) 143°C, $K_1 \begin{array}{l} \rightarrow K_2 \\ \searrow N \end{array}$; (*c*) 143°C, $N \rightsquigarrow K_2$; (*d*) 146°C, $K_2 \rightarrow N$.

2.8. *Double melting behaviour via the nematic phase in* $(C_4O\text{–}DTB)(C_4O\text{–}PTB)Ni$

The $(C_4O\text{–}DTB)(C_4O\text{–}PTB)Ni$ complex **3a** also exhibits double melting behaviour via the nematic phase. A series of photomicrographs in figure 12 shows the double melting behaviour observed for this complex.

Figure 12(*a*): a mixture of K_1 and K_2 crystals could be obtained at room temperature on cooling the nematic phase from 150°C with an appropriate cooling rate. In this photograph a small strip-like K_2 crystal was surrounded by a big K_1 spherulite.

Figure 12(*b*): when the mixture in figure 12(*a*) was heated up to 143°C between the m.p. of the K_1 crystal (139°C) and that of the K_2 crystal (145°C), the K_1 spherulite transformed into the strip-like K_2 crystals and the remaining portion of the K_1 spherulite melted into the nematic phase.

Figure 12(*c*): after holding the temperature at 143°C for 5 min, all portions of the K_1 spherulite completely melted into the nematic phase, which was slowly recrystallized into the strip-like K_2 crystals by the relaxation.

Figure 12(*d*): when the sample in figure 12(*c*) was heated up to 146°C over the m.p. (145°C) of the K_2 crystals, the strip-like crystals completely melted into the nematic phase.

Thus, the $(C_4O\text{–}DTB)(C_4O\text{–}PTB)Ni$ complex exhibits a double melting behaviour via the nematic phase.

This unique double melting behaviour could also be observed by the DSC measurements. Figure 13 shows typical thermograms of the double melting behaviour [19] for this complex. In this figure a small shoulder I at 131°C corresponds to the

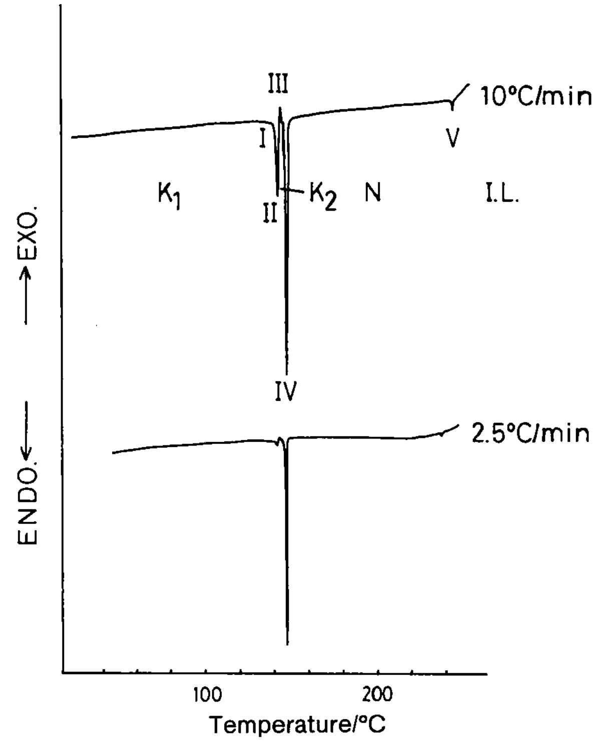

Figure 13. DSC thermograms of the $(C_4O\text{–}DTB)(C_4O\text{–}PTB)Ni$ complex, **3a** for the different heating rates.

crystal–crystal phase transition from the K_1 crystals to the K_2 crystals. Endothermic peaks II (139°C), IV (145°C), and V (242°C) correspond to the melting from the K_1 to the nematic phase, the melting from the K_2 to the N, and the clearing from the N to the isotropic liquid, respectively. The exothermic peak III between peak II and peak IV means the recrystallization from the melt (N) of the K_1 crystals to the K_2 crystals. The ratio of peak II to peak IV decreases with a slower heating rate. This is a characteristic of double melting behaviour [20]. Thus, it was confirmed that the (C_4O–DTB)(C_4O–PTB)Ni complex **3a** exhibits unusual double melting behaviour via the nematic phase. Such a unique double melting behaviour via the nematic phase is the first example in liquid crystals.

The nematic phase in this (C_4O–DTB)(C_4O–PTB)Ni complex, **3a**, was established by a miscibility contact method; the nematic phase is totally miscible with the nematic phase in tetraphtalylidene-bis-4-*n*-butylaniline (TBBA) [21].

2.9. *Reversible transformation between the blue smectogen and the red nematogen*

It should be emphasized that the original ML_2 (M = metal, L = ligand) type of $(C_8O\text{–DTB})_2Ni$ complex **2b** is a deep *blue smectic rod-like* compound, and that, on the other hand, the transformed MLL′ (L ≠ L′, i.e. mixed ligands) type of (C_4O–DTB)(C_4O–PTB)Ni and (C_8O–DTB)(C_8O–PTB)Ni complexes, **3a,b**, are deep *red nematic* Λ-*like* compounds. The complexes **3a** and **3b** are the first liquid crystals in mixed-ligand complexes. Furthermore, **2a,b** and **3a,b** are good dyes because each of them has a very big extinction coefficient, e.g. 22400 at 594 nm for **2b** in $CHCl_3$.

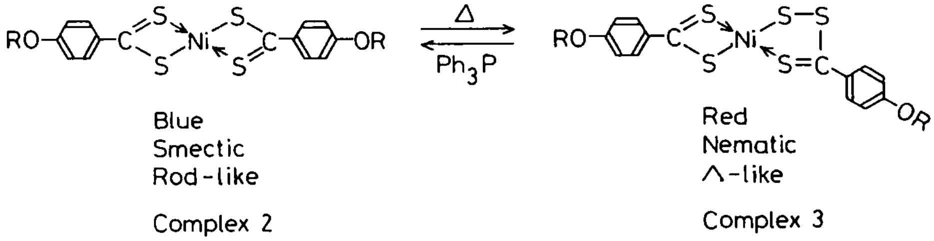

Figure 14. Reversible transformation between the complexes **2** and **3**.

As mentioned previously, the blue smectic rod-like complex (**2**) can be transformed into the red nematic Λ-like complex (**3**) by the intermolecular reactions between the blue complexes (**2**) at 230–285°C. Furthermore, the red Λ-like nematic complex (**3**) in chloroform can easily be transformed back into the original blue rod-like complex (**2**) by adding triphenylphosphine. Therefore, the reversible transformation between the blue smectic rod-like complex (**2**) and the red nematic Λ-like complex (**3**) is possible as illustrated in figure 14, although the amount of the transformation from the blue to the red decreases by the degradation as shown in figure 8. Such a unique transformation of these present mesogens is the first example in liquid crystals.

3. Conclusion

It was found that the long-chain-substituted bis(dithiobenzoato)nickel(II) complex, $(C_nO\text{–DTB})_2Ni$ for $n = 8$, has *smectic* H and C mesophases, and that the $(C_nO\text{–DTB})_2Ni$ complexes for $n = 4$ and 8 easily transform into the corresponding monoperthio complexes, (C$_n$O–DTB)(C$_n$O–PTB)Ni, by heating at temperatures between 230°C and 285°C. It was confirmed that the transformation originates from an intermolecular reaction between the (C$_n$O–DTB)$_2$Ni complexes at high temperatures, and that the origin of the extra sulphurs in the resulting (C$_n$O–DTB)(C$_n$O–PTB)Ni complexes is the neighbouring (C$_n$O–DTB)$_2$Ni complexes. Interestingly, each of the monoperthio complexes, (C$_n$O–DTB)(C$_n$O–PTB)Ni (n = 4 and 8), exhibits *nematic* mesomorphism and a unique double melting behaviour via the nematic phase, which is the first example in liquid crystals. The reversible transformation between the *blue smectic rod-like* (C$_n$O–DTB)$_2$Ni complex and the *red nematic* Λ-*like* (C$_n$O–DTB)(C$_n$O–PTB)Ni complex is possible.

4. Experimental

4.1. *Measurements*

The phase transition behaviour of these complexes was observed by a polarizing microscope equipped with a heating plate controlled by a thermoregulator, Mettler FP80 and FP82, and measured with a differential scanning calorimeter, Rigaku Thermoflex TG-DSC. X-ray diffraction powder patterns of the phases of these complexes were measured with Cu-Kα radiation, using a Rigaku Geigerflex equipped with a heating plate controlled by a thermoregulator [22]. The infrared spectra and the ultraviolet-visible spectra were recorded on a JASCO A-302 infrared spectrometer and a Hitachi 330 spectrophotometer, respectively. A Brüker AC-250 spectrometer (250 MHz) was used for FT-^{1}H-NMR spectra.

4.2. *Synthesis*

The bis(*p*-*n*-alkoxydithiobenzoato)nickel(II) complexes, **2**, were prepared by a modification of the method of Bost and Mattox [11]. The (*p*-*n*-alkoxydithiobenzoato)(*p*-*n*-alkoxyperthiobenzoato)nickel(II) complexes, **3**, could be obtained by heating the bis(*p*-*n*-alkoxydithiobenzoato)nickel(II) complexes, **2**, at 230°C. Since the synthetic procedures were almost the same as in the case of the octyl substituent, the detailed procedures are presented here only for the complexes (C$_8$O–DTB)$_2$Ni, **2b**, and (C$_8$O–DTB)(C$_8$O–PTB)Ni, **3b**.

4.3. *Bis*(*p-n-octyloxydithiobenzoato*)*nickel*(*II*), **2b**, (*C$_8$O–DTB*)$_2$*Ni*

Carbondisulphide (1·50 g, 19·3 mmol) at 0°C was added dropwise to a Grignard reagent prepared from *p*-bromo-*n*-octyloxybenzene (5·00 g, 17·5 mmol) in tetrahydrofuran (30 ml), and the reaction mixture was stirred for an additional hour at this temperature. Then a dilute aqueous solution of hydrochloric acid was added to give a red solution. It was extracted with ether, and the organic layer was dried over sodium sulphate. After an evaporation of the ether, 50 ml of ethanol and then nickel(II) dichloride hexahydrate (2·08 g, 8·75 mmol) in 10 ml of ethanol were added to the residue. After stirring 2 hours at room temperature, blue–violet precipitate was formed, filtered, and washed with ethanol to give the crude complex. The purification was performed by a recrystallization from chloroform to afford 2·90 g of dark blue strip-like crystals. Yield 53·3 per cent. IR (KBr pellet, cm^{-1}) 2950, 2870, 1600, 1510, 1260, $\nu_{(\mathrm{CSS})} = 1165$, $\nu_{(\mathrm{C=S})} = 1002$, $\nu_{(\mathrm{Ni\text{-}S})} = 380$. Electronic spectrum (in CHCl$_3$ ($\lambda_{\max}(\log\varepsilon)$)): 290 nm (4·16), 323 (4·19, shoulder), 374 (5·08), 429 (3·98, sh.), 551 (4·12, sh.), 594 (4·35), 6·31 (4·10, sh.), 741 (3·62, sh.). FT-^{1}H-NMR(CDCl$_3$, TMS): δ_{ppm} = 0·89 (t, J = 6·7 Hz, 6 H), 1·25 ~ 1·84 (m, 24 H), 4·04 (t, J = 6·5 Hz, 4 H), 6·88 (d, J = 9·0 Hz, 4 H), 8·04 (d, J = 8·9 Hz, 4 H). Anal. found. (calcd. for $C_{30}H_{42}O_2S_4Ni$): C 57·93 per cent (57·97), H 6·91 per cent (6·81).

4.4. (*p-n-Octyloxydithiobenzoato*)(*p-n-octyloxyperthiobenzoato*)*nickel*(*II*), ***3b***, (*C₈O–DTB*)(*C₈O–PTB*)*Ni*

The $(C_8O\text{–}DTB)_2Ni$ complex (0·14 g) was heated at 230°C for 10 hours. The resulting red compound was recrystallized from *n*-hexane to give 0·062 g of the soft red powder of $(C_8O\text{–}DTB)(C_8O\text{–}PTB)Ni$.

IR (KBr pellet, cm^{-1}): 2950, 2870, 1600, 1510, 1260, $\nu_{(CSS)}$ = 1165, $\nu_{(SS)}$ = 530. Electronic spectrum (in $CHCl_3$ (λ_{max} (log ε))): 361 nm (4·81), 438 (3·89), 526 (4·16), 554 (sh., 4·13). FT-^{1}H-NMR ($CDCl_3$, TMS): δ_{ppm} = 0·89 (t, J = 7·2 Hz, 6 H), 1·24–1·88 (m, 24 H), 4·01 (t, J = 6·4 Hz, 2 H), 4·05 (t, J = 6·4 Hz, 2 H), 6·86 (d, J = 9·0 Hz, 2 H), 6·92 (d, J = 9·0 Hz, 2 H), 7·89 (d, J = 8·9 Hz, 2 H), 8·06 (d, J = 8·9 Hz, 2 H). Anal. found. (calcd. for $C_{30}H_{42}O_2S_3Ni$): C 54·87 per cent (55·12), H 6·42 per cent (6·48).

This work was supported in part by a Grant-in-Aid for Scientific Research (No. 01750755) from the Ministry of Education, Science, and Culture.

References

[1] Chamberlain, C. S., and Drago, R. S., 1979, *Inorg. chim. Acta*, **32**, 75.

[2] Drago, R. S., Desmond, M. J., Corden, B. B., and Miller, K. A., 1983, *J. Am. chem. Soc.*, **105**, 2287.

[3] Humphry-Baker, R., Moroi, Y., Grätzel, M., Pelizzeitti, E., and Tundo, P., 1980, *J. Am. chem. Soc.*, **102**, 3689. Markovitsi, D., Knoesel, R., and Simon, J., 1982, *Nouv. J. Chim.*, **6**, 531.

[4] Sato, M., Nakahara, H., Fukuda, K., and Akabori, S., 1988, *J. chem. Soc. Chem. Commun.*, p. 24.

[5] (a) Double melting behaviour via an isotropic liquid which we call 'usual double melting behaviour': Ohta, K., Yokoyama, M., and Mikawa, H., 1980, *J. chem. Soc. Chem. Commun.*, p. 392. Ohta, K., Jiang, G.-J., Yokoyama, M., Kusabayashi, S., and Mikawa, H., 1981, *Molec. Crystals liq. Crystals*, **66**, 283. Ohta, K., Yokoyama, M., Kusabayashi, S., and Mikawa, H., 1981, *Molec. Crystals liq. Crystals*, **69**, 131. Ohta, K., Muroki, H., Hatada, K., Yamamoto, I., and Matsuzaki, K., 1985, *Molec. Crystals liq. Crystals*, **30**, 249. (b) The first double melting behavior via a mesophase which we call 'unusual double melting behaviour': Ohta, K., Ema, H., Muroki, H., Yamamoto, I., and Matsuzaki, K., 1987, *Molec. Crystals liq. Crystals*, **147**, 61.

[6] Giroud, A. M., and Mueller-Westerhoff, U. T., 1977, *Molec. Crystals liq. Crystals Lett.*, **41**, 11. Piechocki, C., Simon, J., Skoulios, A., Guillon, D., and Weber, P., 1982, *J. Am. chem. Soc.*, **104**, 5245. Ohta, K., Ishii, A., Yamamoto, I., and Matsuzaki, K., 1984, *J. chem. Soc. Chem. Commun.*, p. 1099.

[7] Trech, P., Chachaty, C., Gaillard, J., and Giroud-Godquin, A. M., 1987, *J. Phys., Paris*, **48**, 663. Ohta, K., Watanabe, T., Fujimoto, T., and Yamamoto, I., 1989, *J. chem. Soc. Chem. Commun.*, p. 1611.

[8] Ohta, K., Muroki, H., Takagi, A., Hatada, K., Ema, H., Yamamoto, I., and Matsuzaki, K., 1986, *Molec. Crystals liq. Crystals*, **140**, 131. Ohta, K., Takagi, A., Muroki, H., Yamamoto, I., Matsuzaki, K., Inabe, T., and Maruyama, Y., 1987, *Molec. Crystals liq. Crystals*, **147**, 15.

[9] Ohta, K., Ema, H., Yamamoto, I., and Matsuzaki, K., 1988, *Liq. Crystals*, **3**, 1671.

[10] See [5(b)].

[11] Bost, R. W., and Mattox, W. J., 1930, *J. Am. chem. Soc.*, **52**, 332.

[12] Gray, G. W., and Goodby, J. W., 1984, *Smectic Liquid Crystals* (Leonard Hill), pp. 107 and 121.

[13] See figure 2 in: Helfrich, W., 1979, *J. Phys., Paris, Colloq.*, **40**, C3–105. The smectic G and H phases in this paper correspond to the smectic H and G phases denoted by Gray and Goodby in [12], respectively.

[14] FACKLER, J. P., JR., COUCOUVANIS, D., FETCHIN, J. A., and SEIDEL, W. C., 1968, *J. Am. chem. Soc.*, **90**, 2784.
[15] FURLANI, C., FLAMINI, A., SGAMELLOTTI, A., and BELLITTO, C., 1973, *J. chem. Soc. Dalton*, p. 2404.
[16] FACKLER, J. P., JR., and COUCOUVANIS, D., 1967, *J. Am. chem. Soc.*, **89**, 1745.
[17] See figure 6: COUCOUVANIS, D., and FACKLER, J. P., JR., 1967, *J. Am. chem. Soc.*, **89**, 1346.
[18] The multiple melting behaviour of glycerides is well known: CHAPMAN, D., 1962, *Chem. Rev.*, **62**, 433.
[19] See figure 7 in [18].
[20] See figure 2 in [5 (b)].
[21] See [12], pp. 20.
[22] EMA, H., 1988, Master thesis, Shinshu University, Chap. 7.